International Journal of Design & Nature and Ecodynamics
Vol. 20, No. 6, June, 2025, pp. 1295-1312
Journal homepage: http://iieta.org/journals/ijdne

Analysis of Hydrological Characteristics and Rainfall Distribution Patterns in the Cimanuk River Basin, West Java, Indonesia

Nicco Plamonia[1,2,3*], Dwi Aryani[2], Atie Tri Juniati[3], Nabila Seknun[2], Ahmad Pratama Putra[4], Ikhsan Budi Wahyono[1], Mohammad Zaidan[5], Bambang Winarno[5], Budi Kurniawan[5], Prihartanto[1]

[1] Research Center for Environmental and Clean Technology, National Research and Innovation Agency, South Tangerang 15314, Indonesia
[2] Civil Engineering Department, Faculty of Engineering, Universitas Pancasila, Jakarta 12640, Indonesia
[3] Infrastructure and Environmental Engineering Department, Universitas Pancasila, Jakarta 12640, Indonesia
[4] Geological Disaster Research Center, National Research and Innovation Agency, Jakarta 10340, Indonesia
[5] Research Center for Limnology and Water Resources, National Research and Innovation Agency, Jakarta 10340, Indonesia

Corresponding Author Email: nicco.plamonia@brin.go.id

https://doi.org/10.18280/ijdne.200610

Received: 23 March 2025
Revised: 5 June 2025
Accepted: 25 June 2025
Available online: 30 June 2025

Keywords:
Cimanuk River Basin, hydrological characteristics, rainfall distribution, Thiessen Polygon method, SCS-CN method, GIS analysis
runoff prediction, watershed management

ABSTRACT

This study integrates GIS-based spatial analysis with hydrological modelling to assess rainfall distribution and surface runoff potential. Rainfall was interpolated using Thiessen Polygon and Kriging methods, yielding coverage areas of 150,765.37 ha and 132,096.12 ha, respectively. These spatial datasets were then used as inputs in the SCS-CN (Soil Conservation Service Curve Number) model, which incorporates land cover and soil type data to estimate runoff. The resulting CN value of 61.472 indicates moderate runoff, suggesting that approximately 61.5% of rainfall contributes to surface flow, relevant for flood control, retention basin sizing, and erosion mitigation. GIS facilitated the identification of under-monitored areas, revealing that only 6 rainfall stations are currently active, while 13 are recommended by WMO standards. This highlights the need for network expansion to improve data reliability. Overall, this study clarifies the direct application of GIS-derived rainfall zones to hydrological modelling, emphasizing their value in water resource planning and disaster risk reduction within the Cimanuk Basin.

1. INTRODUCTION

A watershed is a land area bounded by mountain ridges where rainwater that falls within this region is naturally collected and channeled through a network of small streams into a main river [1, 2]. Watersheds play a crucial role in regulating hydrological flow, preserving ecological balance, and minimizing soil erosion [3]. However, when a watershed is damaged—through deforestation, poor land-use planning, or other environmental pressures—its ability to regulate water flow is significantly impaired. This degradation can lead to natural disasters such as flooding, landslides, and droughts. For instance, flooding occurs when rainfall exceeds the watershed's capacity to absorb or channel runoff effectively. Therefore, to understand and anticipate such events, accurate rainfall measurement is essential. Rainfall data is typically collected from a network of rain gauge stations within the watershed. The Thiessen Polygon method [4-7] is commonly used to estimate spatial rainfall distribution by assigning weights to each station based on the area it represents. This method involves dividing the watershed into polygons, each centered on a rain station, ensuring equidistance to neighboring stations. The Thiessen constant, calculated as the ratio of each polygon's area to the total watershed area, plays a key role in rainfall interpolation and hydrological analysis.

The Cimanuk River Basin was selected due to several key characteristics that make it highly relevant for hydrological modelling and spatial rainfall analysis:

1. Hydrological Importance: The Cimanuk River Basin spans 3.414,53 km² [8] across multiple districts in West Java, Indonesia. It is a vital water source for agriculture, urban settlements, and industries, making its hydrological behavior crucial for regional planning [9, 10].
2. Complex Environmental Features: The basin presents a diverse mix of land cover, including the rice field area in the Cimanuk Watershed (DAS Cimanuk) covers approximately 128,788.84 hectares, or about 33.22% of the total watershed area. In addition to rice fields, most of the other land uses in the Cimanuk Watershed consist of dry fields (116,960.92 hectares, 30.17%) and mixed gardens (72,533.16 hectares, 18.71%)—with 23 distinct soil types. This heterogeneity creates a challenging and representative case for applying GIS-based hydrological models like SCS-CN and rainfall interpolation techniques [11, 12].
3. Data Gaps and Infrastructure Deficiency: The area currently operates only 6 rainfall stations, whereas the WMO recommends 13 for a watershed of this size

and topographic complexity. This gap justifies the need for assessing spatial rainfall distribution using methods like Thiessen [13] and Kriging [14, 15], highlighting the importance of station placement in hydrological accuracy.

4. Flood Risk and Water Management Relevance: The Cimanuk Basin has a history of flooding during rainy seasons [16-18]. Therefore, insights from this study are expected to support disaster mitigation and improve hydrological resilience in the region.

These factors establish the Cimanuk River Basin as a strategic and scientifically meaningful study area for evaluating the interplay between land characteristics, rainfall distribution, and runoff estimation.

This research contributes directly to water resources management [19-21] and flood risk assessment [22, 23] by providing a detailed spatial analysis of rainfall distribution and hydrological parameters specific to the Cimanuk Watershed. By integrating GIS-based techniques with the Thiessen Polygon method, this study improves the understanding of rainfall variability, which is critical for accurate runoff estimation and flood forecasting. Moreover, this paper innovates by: (1) Evaluating the effectiveness of rain gauge station placement [24, 25] using spatial interpolation techniques, addressing a key data gap identified by WMO standards; (2) Applying the SCS-Curve Number (CN) method tailored to the diverse land use and soil types [26, 27] of the Cimanuk basin, refining runoff predictions [28, 29] compared to prior studies in similar tropical watersheds; (3) Demonstrating the integration of remote sensing data with GIS tools to enhance hydrological modelling accuracy in data-sparse regions, which is increasingly important for watershed management in developing countries [30, 31]. The main research question of this study is: How does the rainfall distribution pattern in the Cimanuk Watershed affect hydrological analysis, and how can GIS be utilized to evaluate the spatial coverage of rain gauge stations in relation to the watershed area?. Accordingly, the main objective of this research is to analyse the spatial distribution of rainfall across the Cimanuk Watershed, evaluate the effectiveness of rain gauge station placement using Geographic Information System (GIS) tools, and determine key hydrological parameters—particularly the Curve Number (CN)—with a specific focus on assessing the relationship between the number and distribution of rainfall stations and the watershed's spatial characteristics.

2. METHOD

This article builds upon the research conducted on the Cimanuk Watershed (See Figure 1), which spans several regencies in West Java, Indonesia, including Garut, Sumedang, Majalengka, Indramayu, and Cirebon [32]. The Watershed plays a significant role in the region's hydrology and flood management [33]. The Cimanuk River originates from the foot of Mount Papandayan in Garut Regency, located at an elevation of approximately 1,200 meters above sea level [34]. The river then flows in a northern direction over a distance of 180 kilometers, ultimately emptying into the Java Sea at the coastal area of Indramayu Regency. The total length of the Cimanuk River, including its tributaries, is approximately 337.67 kilometres [35, 36].

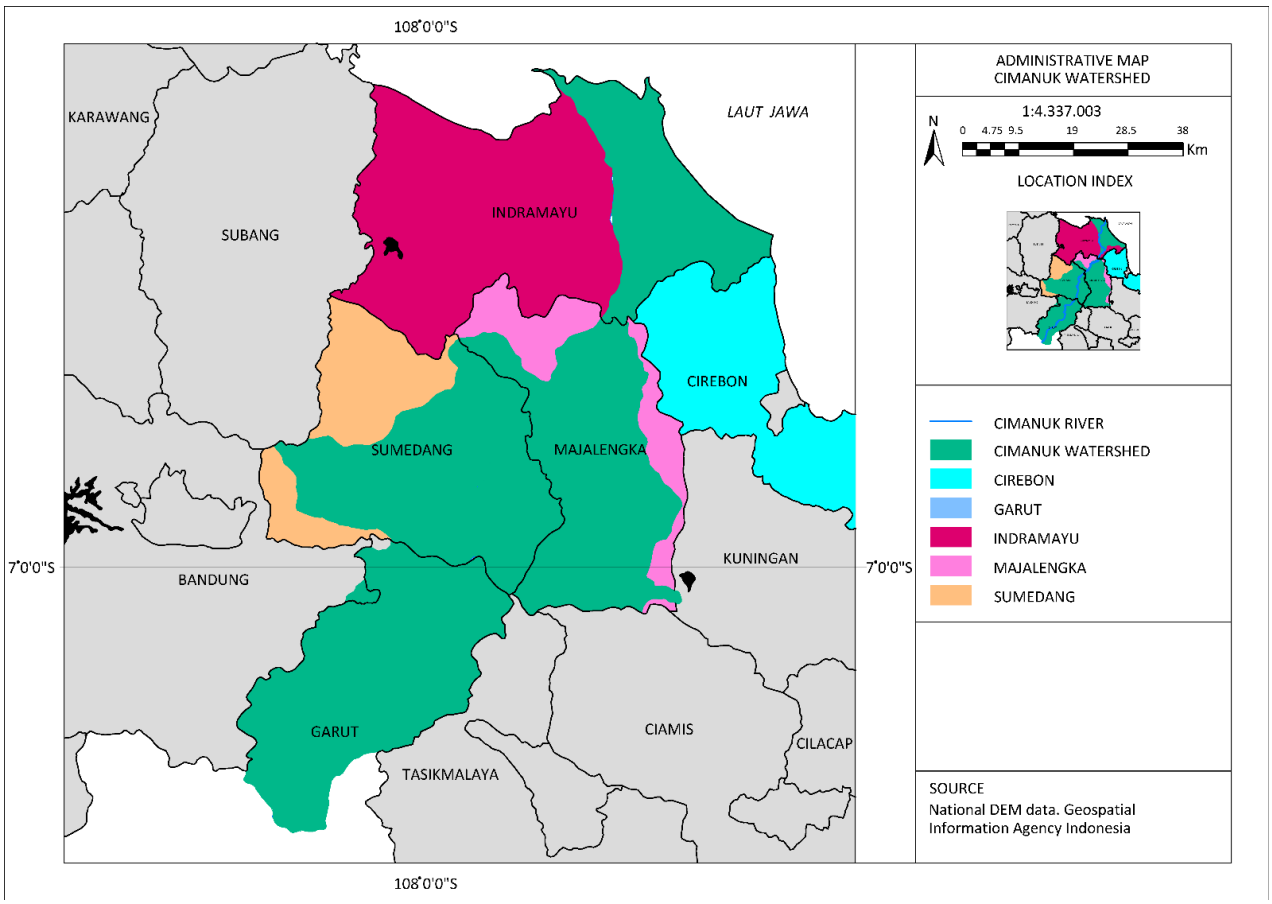

Figure 1. Cimanuk Watershed administrative map

2.1 Research sequences

This research is quantitative, applied, and descriptive in nature [37-39]. This study employs a combination of GIS techniques, statistical methods, and hydrological models. The flowchart of research and data analysis is presented in Figure 2. The process begins by gathering essential data from multiple sources, such as the rainfall data and discharge stations between 2008 and 2018, Digital Elevation Model (henceforth, DEM) data from 2019, rainfall data from 2018, land use data from 2011, and soil data. These datasets are essential for understanding the topography, land cover, and hydrological behaviour of the watershed. Next, the study uses GIS techniques to overlay and analyse the data. This includes overlaying the watershed area with the sub-watershed data, as well as integrating the rainfall data with land use data to identify patterns in rainfall distribution and land cover types. The study then applies the Thiessen Polygon and Kriging methods to analyse the rainfall data, providing insights into the spatial distribution of rainfall and identifying areas with insufficient coverage by rain stations. Additionally, the Rational Method is used to evaluate the watershed's hydrological characteristics and estimate runoff potential. The study also calculates the CN value for the watershed using the SCS-CN method, which is a critical factor for flood risk management and water resource planning. By employing these methodologies, the study aims to provide a comprehensive understanding of the Cimanuk Watershed's hydrology, allowing for more accurate predictions and informed decision-making regarding water resource management [40] and flood control.

In Section 2.2, we will explain the sequence of analysing data employing and combining several methods in conducting this research, to determine the characteristics and rainfall distribution patterns within the Cimanuk Watershed.

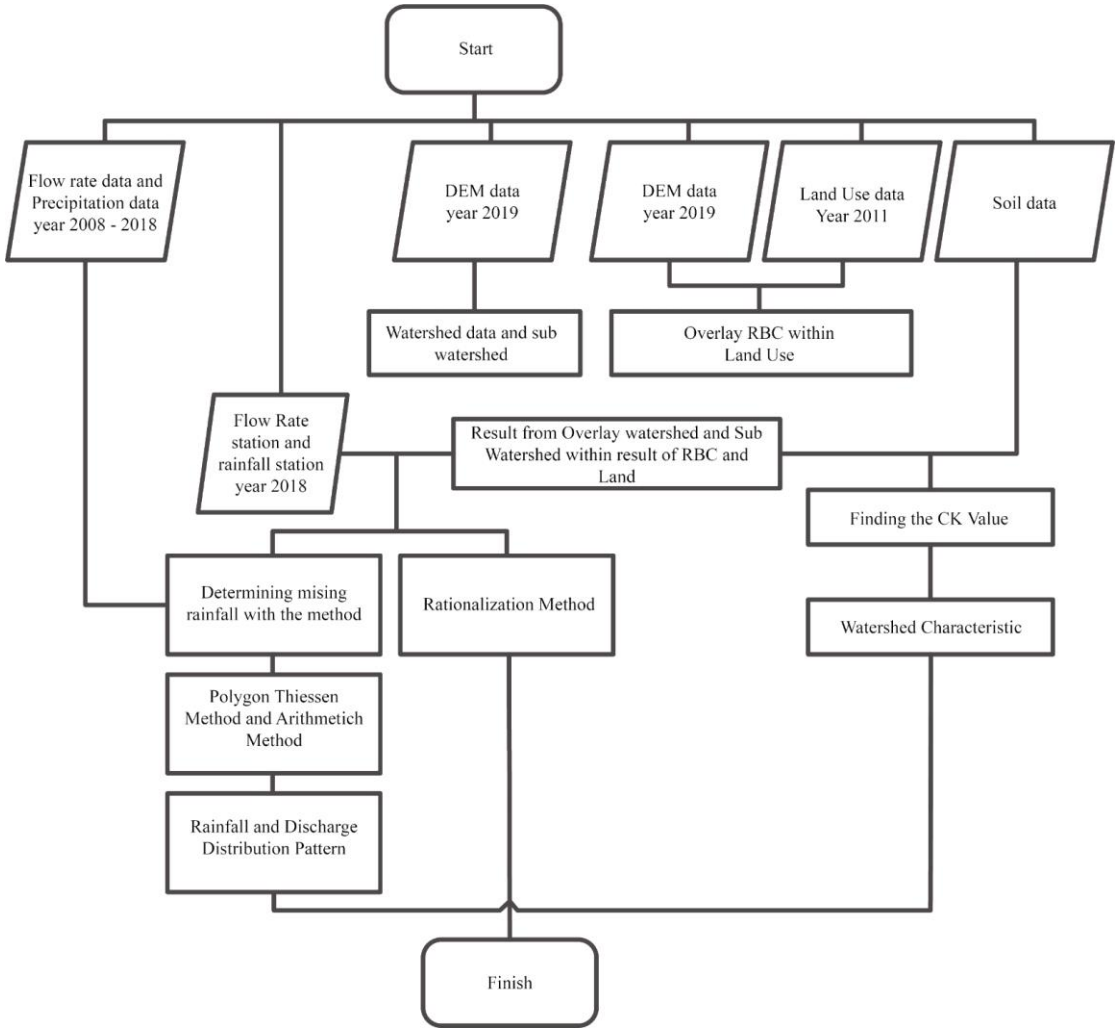

Figure 2. Research sequences

2.2 Analysis of digital elevation model, land cover, soil, sub-watershed, and data overlay

As mentioned in Section 2.1, several steps were undertaken to analyse various aspects of the Cimanuk Watershed using GIS and other spatial data to gain a comprehensive understanding of the watershed's characteristics. These steps were crucial in providing a comprehensive spatial understanding of the Cimanuk Watershed. The combination of DEM data, land use, soil characteristics, slope analysis, and sub-watershed delineation enabled more accurate predictions and assessments of rainfall behaviour, flood risks, and land use impacts within the watershed. Moreover, the detailed explanation of the methodology is crucial in this study to ensure clarity, transparency, and reproducibility of the research:

(1) Creating a Cimanuk Watershed Map using DEM Data: DEM data is involved in order to create a map of the

Cimanuk Watershed. The Cimanuk Watershed map allowed for an understanding of the topography of the watershed, including elevation changes, slopes, and river flow patterns. Moreover, DEM data is critical for analyzing how water moves through the landscape and is a fundamental input for hydrological modeling [41].

(2) Creating a Land Use Map: Creating a land use map of the Cimanuk Watershed. This map helped to examine the spatial distribution of vegetation and human activities such as agriculture, settlements, and industrial areas. Understanding land use is essential for hydrological modelling, as different land uses affect runoff, water infiltration [42], and erosion [43, 44].

(3) Creating a Soil Map: A soil map was created for the watershed. This map is critical for analysing the soil types in the region and understanding their potential for erosion and water retention. Different soil types have varying levels of permeability, which impacts how water is absorbed or flows over the surface, affecting the risk of surface runoff and soil erosion [45, 46].

(4) Creating a Slope Map from DEM Data: A slope map helps identify areas with steep slopes that are susceptible to erosion and influences how water flows across the watershed. Areas with steep slopes tend to have higher erosion risks, while flatter areas are more prone to surface runoff during heavy rainfall. The slope map is essential for understanding water movement and designing erosion control strategies [47, 48].

(5) Generating a Sub-Watershed Map: A sub-watershed map was generated using the DEM data. This map divides the Cimanuk Watershed into smaller, more manageable sub-catchments, each with its own unique hydrological characteristics [49]. By breaking the watershed into sub-catchments, it becomes easier to study specific areas and manage water resources and flood risks more efficiently [50].

(6) Performing Overlay Analysis: Overlay analysis was conducted where the boundaries of the Sub-watershed were combined with the land use and slope maps. This analysis provided a detailed map showing both land use types and the slope gradient within each sub-watershed. By overlaying these data layers, the analysis helped to visualize areas with high erosion potential or those most affected by human activities, facilitating better decision-making for land use planning and flood risk management.

By outlining each step taken, from the creation of maps to overlay analysis, the methodology not only allows for a comprehensive understanding of the Cimanuk Watershed but also ensures the reliability of the findings. The integration of multiple data layers and the use of established hydrological models provides a scientifically rigorous approach, making the research valuable for informed decision-making in land use and flood risk management.

2.3 Analysis of rainfall distribution pattern

The analysis of the rainfall distribution pattern consists of several important steps to ensure accurate representation of rainfall behavior. Initially, missing rainfall data was corrected using the Normal Ratio Method to estimate the missing values based on nearby stations with similar rainfall patterns. Following this, two interpolation methods, Kriging and Thiessen Polygon, were used to analyze and map the rainfall distribution within the watershed. These methods were selected to allow a comparative analysis of the results and provide insights into how each interpolation technique influences the rainfall distribution. The primary goal of this comparison is to identify the most accurate method for assessing the rainfall patterns in the region. Further explanations of these methods and their applications in the analysis are provided in Sections 2.3.1, 2.3.2, and 2.3.3.

2.3.1 Ratio normal ratio method

The Normal Ratio Method is a technique used to estimate missing rainfall data at a station where data is unavailable for a particular period. This method is relatively simple, as it calculates the ratio between the missing rainfall at the station in question and the rainfall at nearby stations that have historical data, considering the annual rainfall recorded at each station (See Eq. (1)).

$$\frac{P_x}{N_x} = \frac{1}{n}\left(\frac{P_1}{N_1} + \frac{P_2}{N_2} + \cdots + \frac{P_n}{N_n}\right) \quad (1)$$

where, P_x is missing rainfall at station x (the value to be predicted); $P_1, P_2, \ldots, P_n$ are rainfall data at nearby stations of x for the same period; N_x is annual rainfall at station x (normal annual value for station x); $N_1, N_2, \ldots, N_n$ are annual rainfall at stations surrounding station x; n are Number of rainfall stations used for the calculation around station x.

Steps involved in this method are: (1) Collect annual rainfall data from nearby stations that have complete data for the period; (2) Calculate the ratio between the annual rainfall at station x and the annual rainfall at nearby stations; (3) Use this ratio to estimate the missing rainfall at station x. Therefore, the Normal Ratio Method can be used to fill in missing rainfall data at stations where data is missing for certain periods in a relatively simple and quick manner.

2.3.2 Krigging method

Kriging is an advanced geostatistical interpolation technique used to predict the value of a variable at unsampled locations based on known values from nearby points. It assumes that the spatial correlation between observed data points follows a known structure, called the variogram or semi-variogram, which quantifies the spatial variability of the data (See Eq. (2)).

$$Z_{(S_0)} = \sum_{i=1}^{n} \lambda_i Z_{(S_i)} \quad (2)$$

where, $Z_{(S_0)}$ is the predicted value at an unsampled location S_0; $Z_{(S_i)}$ is the observed value at the sample point sis_isi; λ_i are the weights assigned to each sample point S_i, which are determined by the spatial correlation between the sample points; n is the number of sample points used to estimate the value at S_0. The weights λ_i are derived by solving a system of equations based on the variogram model, which is a key component of Kriging. The variogram model defines how the spatial correlation decreases with distance and is used to calculate the optimal weights for the Kriging interpolation.

The steps for using the Kriging method in GIS are as follows: (1) Input the watershed map data to be used; (2) Input the coordinate data for the station locations; (3) Use the Arc Toolbox attribute; (4) Select the Spatial Analyst Tools menu, then choose Interpolation; (5) Click on the Kriging menu; (6)

The Kriging menu will appear; input the point features according to the required data; (7) In the Z value field, select the data you wish to analyse; (8) Then, in the output surface raster, choose the location where you want to save the result; (9) Finally, click OK to complete the process.

2.3.3 Thiessen Polygon

Thiessen Polygon is one of the most commonly used methods for calculating the average rainfall over a specific area [5, 6]. However, it has some limitations, primarily because it does not take topography into account. The Thiessen Polygon method assumes that each measurement point within a region influences a specific area, and this area represents the correction factor for the rainfall measurement at that point, transforming it into the rainfall value for the corresponding area. Using Arc Toolbox in ArcGIS, Thiessen Polygons can be created to represent the areas of influence for each rain gauge station. These polygons divide the area such that each polygon corresponds to the area most influenced by its respective rain gauge (See Eq. (3)).

$$R = \frac{R_1 . a_1}{A_1} + \frac{R_2 . a_2}{A_2} + \cdots + \frac{R_n . a_n}{A_n} \quad (3)$$

where, R is Average rainfall (mm) over the area; $R_1, R_2, \ldots, R_n$ are Rainfall at each individual rain gauge station (mm); $a_1, a_2, \ldots, a_n$ is area of each polygon (km²) corresponding to each rain gauge station; A_1, A_2, …, A_n are the total areas corresponding to each station's polygon.

The rainfall R is calculated as a weighted average, where the rainfall values $R_1, R_2, \ldots, R_n$ from the individual stations are weighted by the areas they represent. $a_1, a_2, \ldots, a_n$ are the polygon areas created by methods such as Thiessen Polygons, which define the area of influence for each rain gauge. A_1, A_2, …, A_n are the total areas corresponding to each station's polygon, and they should ideally sum up to the total area of the watershed. While the steps to Create a Thiessen Polygon Map: (1) Input the watershed map data that you will use for the analysis; (2) Input the coordinate data for the rain gauge stations (station locations); (3) Open the Search menu, then search for Thiessen Polygon; (4) Select the menu option Create Thiessen Polygon; (5) The Create Thiessen Polygons window will appear; (6) In this window, input the feature data required for the polygon creation; (7) Next, input the output feature class and select the location where you want to save the resulting file; (8) Finally, click OK to generate the Thiessen Polygons.

2.4 Soil conservation service curve number analysis

The SCS-CN method is used to estimate the amount of surface runoff based on land characteristics, land use, and soil moisture conditions during rainfall. The CN value is the key parameter in this calculation. This method is widely used in hydrology to predict surface runoff, particularly in areas with limited data. Below is a detailed explanation, including the formula, assumptions, and analysis steps:

2.4.1 Basic concept of SCS-CN method

The SCS-CN method assumes that the amount of surface runoff (runoff) depends on two main factors: (1) the Soil's ability to absorb water, which is influenced by soil type and land cover; (2) the Soil moisture condition at the time of rainfall (whether the soil is dry, normal, or wet).

2.4.2 CN calculation formula

To calculate the surface runoff (Q) using the SCS-CN method, the following formula is used (See Eq. (4)):

$$Q = \frac{(P - 0.2S)^2}{P + 0.8S} \quad (4)$$

where, Q is surface runoff (mm); P is total rainfall (mm); S is soil absorption capacity (loss) in mm.

To calculate the value of *S*, the following formula is used (See Eq. (5)):

$$S = \frac{25400}{CN} - 254 \quad (5)$$

where, S is soil absorption capacity in mm; *CN* is Curve Number, which is calculated based on soil type, land use, and soil moisture conditions.

2.4.3 CN calculation process

The CN value is determined based on three main factors (see Table 1): (1) Soil Type: Group the soils based on their water absorption capacity [51], categorized into groups A, B, C, and D; (2) Land Use: The type of land cover (e.g., forest, agricultural land, or urban areas) influences the CN value [52, 53]. For example, open land with vegetation will have a lower CN value compared to areas with concrete or asphalt; (3) Soil Moisture: Based on soil moisture condition (dry, normal, or wet), the CN value will vary. Wet soil conditions tend to generate more runoff.

Table 1. CN values for various combinations of soil type, land use, and soil moisture conditions

Soil Group	Land Use	Soil Moisture	CN Value
A	Forest or grassland	Normal	30-60
B	Agricultural land	Wet	60-75
C	Urban areas	Dry	75-85
D	Clay or flooded land	Wet	85-100

CN calculation steps are as follows: (1) Overlay of soil and land use data with land use maps. The land use map provides information on how the land is used (e.g., for agriculture, forest, or urban development), which affects the CN value; (2) CN value analysis based on sub-watershed: Once the overlay is completed, each area within the Sub-Watershed can be analyzed to determine the CN value based on the combination of land use and soil type. The resulting map provides a detailed overview of the soil characteristics in each land cover area, which is then used to calculate the CN value.

2.4.4 Assumptions in the SCS-CN method

(1) Soil Moisture: The method assumes that soil moisture influences the amount of water the soil can absorb. Wet soils (e.g., after prior rainfall) will have higher CN values, resulting in greater surface runoff.
(2) Land Use: Urbanization or intensive agriculture can increase runoff due to reduced water absorption by the soil.
(3) Rainfall Data: Accurate rainfall data is essential for the calculations and should be obtained from the nearest rain stations or reliable weather models.

2.4.5 Evaluation of results

After calculating the CN value for each area, the results are

used to estimate the volume of surface runoff during a given rainfall event. The higher the CN value, the greater the potential for surface runoff, which can increase the risk of flooding. Example Calculation, For an area with a CN value of 75 and a rainfall of P=100, we can calculate the surface runoff (Q): (1) Calculate S, $S = \frac{25400}{CN} - 254 = \frac{25400}{75} - 254 = 240.53$ mm ; (2) Using the SCS-CN formula to calculate Q, $Q = \frac{(P - 0.2S)^2}{P + 0.8S} = \frac{(100 - 0.2\,(240.53))^2}{100 + 0.8\,(240.53)} = \frac{(100 - 48.11)^2}{100 + 192.42} = \frac{(51.89)^2}{292.42} = 9.08$ mm. The result indicates that 9.08mm of the rainfall will become surface runoff in this area.

2.5 Parameter selection and classification criteria for SCS-CN method

The Curve Number (CN) values used in this study were determined using the SCS-CN method, as developed by the USDA Soil Conservation Service (now NRCS) in Technical Release 55 (TR-55). The method integrates land use/land cover (LULC) data and Hydrologic Soil Groups (HSG) to assign CN values, which represent runoff potential.

Land Cover Classification: Land use/land cover classes were obtained from satellite imagery and classified into several categories (e.g., rice fields, dryland agriculture, forest, settlements).

Soil Type Classification: Soil types were identified in the watershed and grouped into four HSG categories (A–D) based on their infiltration capacity, following NRCS guidelines.

Curve Number Assignment: CN values were assigned using standard tables from TR-55 based on combinations of land cover and HSG [54, 55]. The assumption of normal antecedent moisture condition (AMC II) was used throughout the study. The spatial overlay of soil and land cover in GIS produced CN values at the sub-watershed level.

2.6 World Meteorological Organization (WMO)

In general, the rainfall area is larger than the area represented by the rain gauge station, or vice versa. Therefore, considering economic, topographic, and other factors, rain stations must be placed with an optimal density that can provide good data for subsequent analysis. For this purpose, the World Meteorological Organization (WMO) recommends the following minimum density for the rain station network, see Table 2.

Table 2. Network density according to WMO

No.	Type	Area (km²) per Station	
		Normal Condition	Difficult Condition
1	Tropical, Mediterranean, and Temperate Lowland Areas	600-900	3000-9000
2	Tropical, Mediterranean, and Temperate Mountainous Areas	100-250	1000-5000
3	Small Island Mountainous Areas with Variable Rainfall	140-300	
4	Arid and Polar Regions	1500-10000	

Source: Study [50]

The network density is based on both technical and economic aspects of the respective area, in order to achieve an optimal network density that aligns with the socioeconomic value of the data or the required level of accuracy. Each existing rain station network should be regularly reviewed at each operational period to enhance its quality.

3. RESULTS AND DISCUSSION

In this section, the characteristics of the Cimanuk Watershed (DAS) are analyzed based on various parameters. This section is divided into two parts: 3.1 Results and 3.2 Discussion.

3.1 Results

This section provides an in-depth analysis of the spatial characteristics, highlighting key features with specific data on various districts such as Garut, Sumedang, and Cirebon. This section focuses on the physical and environmental characteristics of the Cimanuk Watershed. The analysis of sub-watersheds breaks down the watershed into smaller units to understand local variations in hydrology, soil type, and slope analyses [56], while the land cover analysis outlines the distribution of forests, agriculture, and settlements, providing insights into the impacts of human activity on the watershed. It gives further context to the area's vulnerability to erosion and suitability for development.

3.1.1 Physical and environmental characteristics of the Cimanuk Watershed

Catchment Area Analysis

The catchment area of a watershed significantly impacts the surrounding topography. Table 3 and Figure 3 present the area of the catchment across various regions, showing the contribution of each district to the overall size of the watershed. The detailed distribution of catchment areas allows for better understanding of how different areas contribute to the overall hydrological behavior of the watershed [57].

Table 3. Catchment area of the Cimanuk Watershed

No.	District	Area (Ha)
1	Bandung	2044.60
2	Ciamis	550.80
3	Garut	116642.45
4	Indramayu	47556.94
5	Kuningan	308.58
6	Majalengka	98873.99
7	Subang	6.93
8	Sumedang	104569.43
9	Tasikmalaya	147.20
10	Bendungan Jatigede	72.45
Total		370,773.37

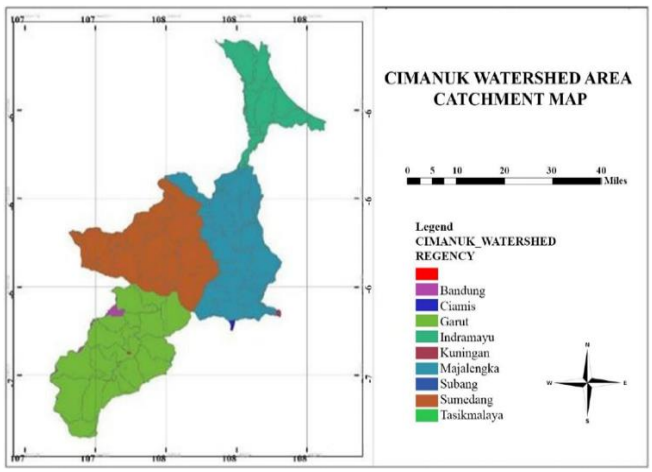

Figure 3. Cimanuk Watershed catchment area map

Sub-Watershed Analysis

Sub-Watershed Analysis identifies the number and area of sub-watersheds within the Cimanuk Watershed. Using GIS software and 8m resolution data, the areas of each sub-watershed were calculated, though some discrepancies arose between the GIS results and the figures provided by the Cimanuk-Cisanggarung River Basin Management Authority. Table 4 presents the areas of each sub-watershed in hectares, offering insights into the spatial distribution and hydrological variations across smaller sub-units (Figure 4).

Table 4. Area of sub-watersheds in the Cimanuk Watershed

Sub-Watersheds	Area (ha)	Sub-Watersheds	Area (ha)
1	6911.28435	19	0.00688511
2	14322.8541	20	12298.273
3	2754.41591	21	8061.79757
4	53.9981773	22	7735.77315
5	0.00471736	23	42868.4653
6	0.0047172	24	0.00471337
7	0.00471694	25	23495.3787
8	0.00471693	26	8698.28905
9	1116.04348	27	11732.7824
10	102.568314	28	0.00471342
11	0.00471784	29	46280.6222
12	0.00471663	30	0.00471381
13	991.421411	31	19625.4448
14	19567.0966	32	9147.4354
15	3573.72924	33	7808.21113
16	3032.6321	34	39296.3961
17	0.0047199	35	8137.22901
18	11229.6482	36	18557.5738
	63655.7249		263743.693
Total		327399.4176	

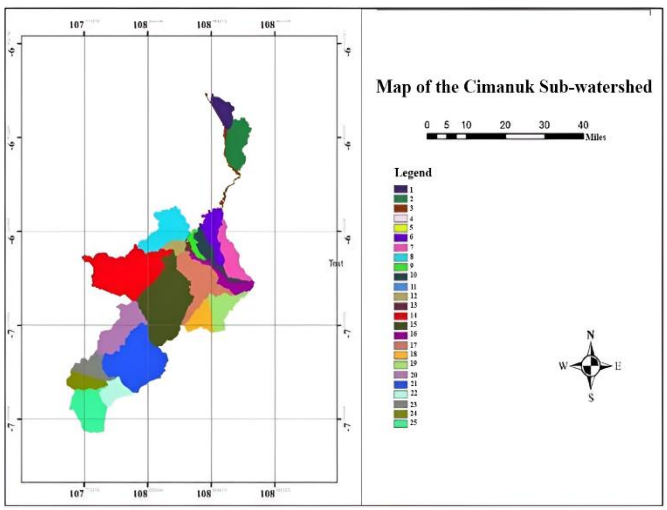

Figure 4. Cimanuk sub-watershed map

Land Cover Analysis

The analysis of land cover is essential to understanding the human impact and natural conditions of a watershed [58, 59]. In the Cimanuk Watershed, GIS software was used to classify land cover into 12 distinct types. The distribution of these land covers, including forests, settlements, and agricultural areas, provides valuable insights into the land-use patterns within the watershed. Table 5 and Figure 5 show the area and percentage of each land cover type.

Table 5. Land cover area of Cimanuk Watershed

No.	Land Cover Type	Area (ha)	Percentage (%)
1	Primary Dryland Forest	2968.36	0.907%
2	Secondary Dryland Forest	12002.19	3666%
3	Plantation Forest	57820.41	17661%
4	Plantation	3776.46	1153%
5	Settlement	26918.31	8222%
6	Dryland Agriculture	80523.84	24595%
7	Dryland Agriculture + Shrubs	38436.42	11740%
8	Rice Fields	95666.80	29220%
9	Shrubs/Bushes	1761.80	0.538%
10	Fish Ponds	4279.72	1307%
11	Open Land	1704.26	0.521%
12	Water Bodies	1540.85	0.471%
	Total Area (Ha)	**327399.42**	**100%**

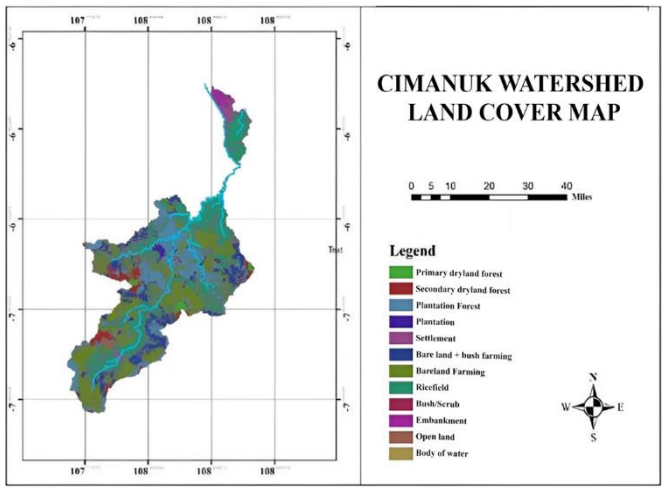

Figure 5. Cimanuk Watershed land cover map

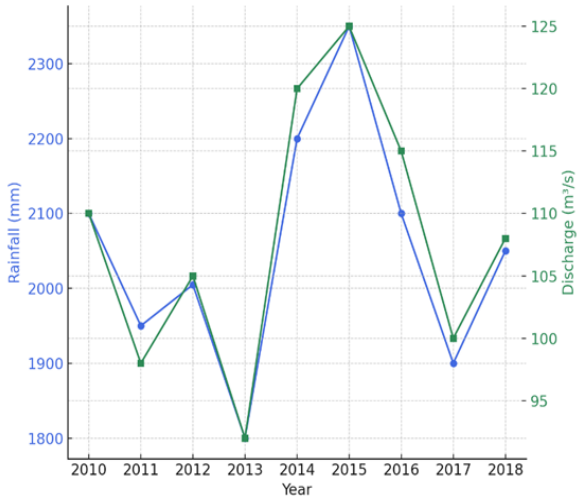

Figure 6. Upward trend in annual discharge

Land Use Change

Land use change plays a critical role in altering the hydrological behavior of a watershed. In the Cimanuk River Basin, the interplay between rainfall patterns, river discharge, and land cover dynamics reflects a gradual transformation of the landscape that has direct implications on runoff generation, infiltration, and flood potential. Due to limited access to multitemporal land cover datasets, this study utilizes a multi-indicator approach to infer land use change trends by integrating: (1) Annual rainfall data from four rainfall stations

across the watershed (2010–2018) (Figure 6); (2) Annual river discharge data ranged from 92m³/s to 125 m³/s (Figure 6); (3) Current land cover proportions as detailed in Table 6 and illustrated in Figure 7.

Table 6. Land cover type

Land Cover Type	Area (ha)	Percentage (%)
Primary Dryland Forest	2,968.36	0.91
Secondary Dryland Forest	12,002.19	3.67
Plantation Forest	57,820.41	17.66
Plantation	3,776.46	1.15
Settlement	26,918.31	8.22
Dryland Agriculture	80,523.84	24.60
Dryland Agriculture + Shrubs	38,436.42	11.74
Rice Fields	95,666.80	29.22
Shrubs/Bushes	1,761.80	0.54
Fish Ponds	4,279.72	1.31
Open Land	1,704.26	0.52
Water Bodies	1,540.85	0.47

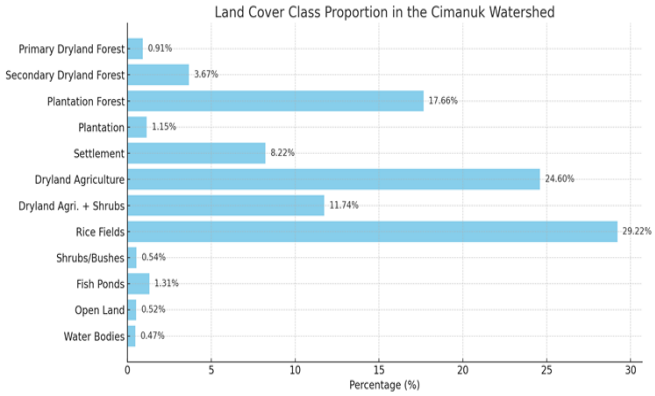

Figure 7. Land cover class proportion in The Cimanuk Watershed

Figure 6 presents the annual rainfall and average river discharge from 2010 to 2018. Rainfall varied between 1,800 mm and 2,350 mm per year. Despite the relatively stable range of annual precipitation, there is a noticeable upward trend in annual discharge, especially between 2014 and 2016. This suggests that factors other than rainfall—most likely land use changes—are contributing to increased runoff generation (See Table 6).

Although this study does not include direct multitemporal land use maps, comparisons with historical reports and regional land cover studies—based on secondary data [60-62]—suggest several notable land use change patterns within the Cimanuk Watershed: (1) Expansion of settlements is evident, with the current built-up area comprising 8.22% of the watershed. Urban development, particularly near the fringes of Garut and Sumedang, has likely increased, reducing infiltration and enhancing surface runoff; (2) There has been a reduction in forested areas, as primary and secondary dryland forests now account for only 4.58% of the total area—relatively low for a basin of this size. The ongoing conversion of these forested areas into plantations and agricultural land continues to alter the natural hydrological balance; (3) A substantial increase in agricultural and mixed-use land is also observed, with rice fields and dryland agriculture together covering over 53% of the watershed. This intensification of agricultural activity is likely contributing to elevated surface runoff and sedimentation during peak rainfall events.

Land Use Change Implications

The current land cover distribution within the Cimanuk Watershed reveals a dominant presence of agricultural and mixed-use land, with dryland agriculture and rice fields accounting for 53.82% of the total area. Settlement areas have expanded to 8.22%, while forest cover—comprising primary and secondary dryland forests—has diminished drastically to just 4.58%. These trends are symptomatic of intensified land use transformation driven by urban and agricultural expansion, especially near urban-rural fringes such as Garut and Sumedang. From a hydrological standpoint, these changes have profound implications. The conversion of forests and natural land to agriculture and settlements reduces vegetative interception, shortens infiltration time, and enhances overland flow. This is especially critical in regions with steep slopes and high rainfall intensity, which are common in the upper watershed. The reduction in canopy cover also leads to increased soil erosion and sediment yield into the river system.

These impacts are corroborated by hydrological data trends: river discharge data from 2014 to 2016 shows a rising trend despite relatively stable rainfall, suggesting that land use change—rather than climatic variation—is the primary driver of increased surface runoff. This observation confirms the ecohydrological disruption caused by uncontrolled land conversion.

The findings highlight the urgency for integrated land and water management approaches, including reforestation in critical recharge areas, enforcement of riparian buffer zones, and zoning regulations to curb unplanned urban sprawl. Without strategic intervention, ongoing land conversion may further exacerbate flood risks, degrade water quality, and undermine the resilience of the watershed system.

Soil Type Analysis

The soil composition within a watershed is crucial for evaluating its erosion risk and suitability for various land uses [63, 64]. In the Cimanuk Watershed, 23 different soil types were identified using GIS analysis. These soil types, ranging from alluvial to andosol soils, exhibit diverse characteristics that influence the hydrological behavior of the region. Table 7 below outlines the areas covered by each soil type within the watershed (See Figure 8).

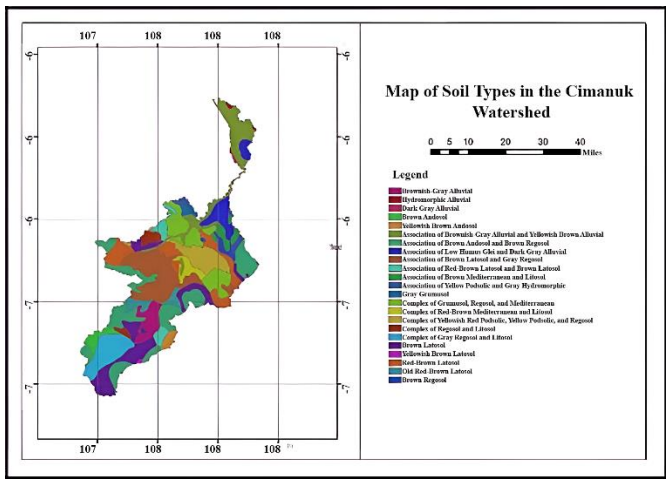

Figure 8. Cimanuk Watershed soil type map

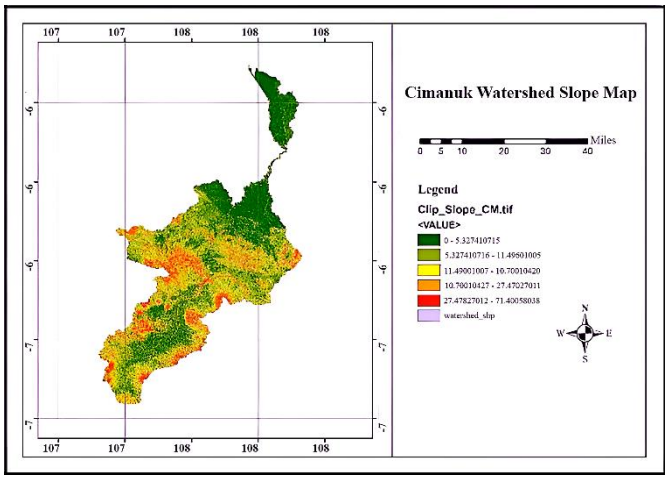

Figure 9. Cimanuk Watershed slope map

Table 7. Soil type area of Cimanuk Watershed

No.	Soil Type	Area (ha)
1	Brownish-Gray Alluvial	11,808.90
2	Hydromorphic Alluvial	725.92
3	Dark Gray Alluvial	573.36
4	Brown Andosol	5,522.60
5	Yellowish Brown Andosol	3,378.04
6	Association of Brownish-Gray Alluvial and Yellowish Brown Alluvial	28,924.30
7	Association of Brown Andosol and Brown Regosol	52,355.40
8	Association of Low Humus Glei and Dark Gray Alluvial	14,397.40
9	Association of Brown Latosol and Gray Regosol	8,161.58
10	Association of Red-Brown Latosol and Brown Latosol	39,124.10
11	Association of Brown Mediterranean and Litosol	5,803.68
12	Association of Yellow Podsolic and Gray Hydromorphic	3,932.21
13	Gray Grumusol	2,560.02
14	Complex of Grumusol, Regosol, and Mediterranean	26,738.30
15	Complex of Red-Brown Mediterranean and Litosol	6,155.12
16	Complex of Yellowish Red Podsolic, Yellow Podsolic, and Regosol	18,129.90
17	Complex of Regosol and Litosol	20,565.30
18	Complex of Gray Regosol and Litosol	5,659.08
19	Brown Latosol	34,794.20
20	Yellowish Brown Latosol	334.39
21	Red-Brown Latosol	26,362.40
22	Old Red-Brown Latosol	7,485.73
23	Brown Regosol	3,907.42
	Total Area	327,399.42

Table 8. Slope area

No.	Slope Classification (%)	Area (Ha)
1	0-5	100818
2	5-25	169755
3	25-45	25758
4	45-55	30917
5	55-72	251
	Total	327500

Slope Analysis

Slope analysis is vital for determining areas prone to erosion and the suitability of land for construction or agriculture [65, 66]. In this study, five slope classifications were identified within the Cimanuk Watershed, each with its own implications for land use and management. Table 8 shows the distribution of slope classes in terms of area, with the largest proportion of the watershed having a slope between 5-25% (see Table 8 and Figure 9).

Analysis of the Rationality of Rainfall Station Density in The Cimanuk Watershed

The current density of rainfall stations in the Cimanuk Watershed, with only six stations covering approximately 3,274 km², is significantly below the WMO recommended density of one station per 100-250 km² for regions with complex topography. This insufficient station density impacts the accuracy of rainfall interpolation, particularly in mountainous areas where precipitation can vary drastically over short distances due to orographic effects. Sparse station distribution limits the capacity to capture local rainfall variability, leading to spatial inaccuracies in the estimation of rainfall input. Such inaccuracies propagate through hydrological models, potentially causing underestimation or overestimation of surface runoff, groundwater recharge, and flood risk. This uncertainty reduces the reliability of model outputs used for water resource planning and disaster mitigation. Therefore, it is critical to increase the number of rainfall stations, especially in high-variability zones identified by topographic and ecohydrological analyses. Enhancing the rainfall monitoring network will reduce spatial uncertainty, improve model calibration, and enable more precise forecasting of hydrological responses, ultimately supporting better watershed management and flood risk reduction in the Cimanuk Watershed.

3.1.2 Analysis of hydrological pattern in the Cimanuk Watershed

This section provides a detailed analysis of hydrological patterns in the Cimanuk Watershed, essential for effective management. It covers: (1) rainfall distribution; (2) the density of rainfall stations (3) Distribution Pattern Analysis Using the Thiessen Polygon Method; (4) Distribution Pattern Analysis Using the Kriging Method; (5) Comparison Between Thiessen and Kriging Methods; (6) Explain related to CN Value Analysis in the Cimanuk Watershed; (7) Analysis of the Rationality of Rainfall Station Density in the Cimanuk Watershed. These results offer insights into hydrological dynamics and help predict surface runoff in the Cimanuk River Basin, guiding future watershed management strategies.

Table 9. Analysis of monthly rainfall data over eight years in the Cimanuk Watershed using the Thiessen Polygon method

Month	Years								
	2010	2011	2012	2013	2014	2015	2016	2017	2018
January	82	214	220	388	143	97	303	422	114
February	87	192	406	390	104	140	392	166	269
March	93	403	213	317	204	179	443	322	124
April	128	218	238	393	124	141	235	262	110
May	324	122	129	266	46	76	166	81	49
June	72	26	41	248	55	28	85	100	40
July	90	66	2	207	57	6	131	43	1
August	62	0	0	11	18	6	147	5	1
September	251	1	2	8	1	0	324	19	3
October	186	76	86	67	15	10	200	156	8
November	365	280	201	184	126	114	258	333	97
December	416	280	440	338	462	294	163	177	139

Rainfall Data Analysis Results

The calculation of rainfall data is aimed at identifying the coverage area of stations with similar rainfall amounts [67,

68]. In this analysis, rainfall data from the Cimanuk Watershed from 2010 to 2018 were evaluated using the Thiessen Polygon method and Microsoft Excel. The analysis focused on data from four rainfall stations over the period of 2010-2018.

Table 9 shows the annual rainfall analysis using the Thiessen Polygon method, with data covering the period from 2010 to 2018. This data helps determine the rainfall distribution over the Cimanuk Watershed during the last eight years.

Figure 10 illustrates the changes in rainfall over the Cimanuk Watershed from 2010 to 2018, based on the Thiessen Polygon method. Below is the list of maximum rainfall events recorded across the four stations in the watershed during these eight years (see Table 10 and Figure 11).

Table 10. Maximum rainfall analysis in the Cimanuk Watershed

Year	Maximum Rainfall (mm)
2010	558
2011	512
2012	529
2013	574
2014	995
2015	494
2016	675
2017	628
2018	512

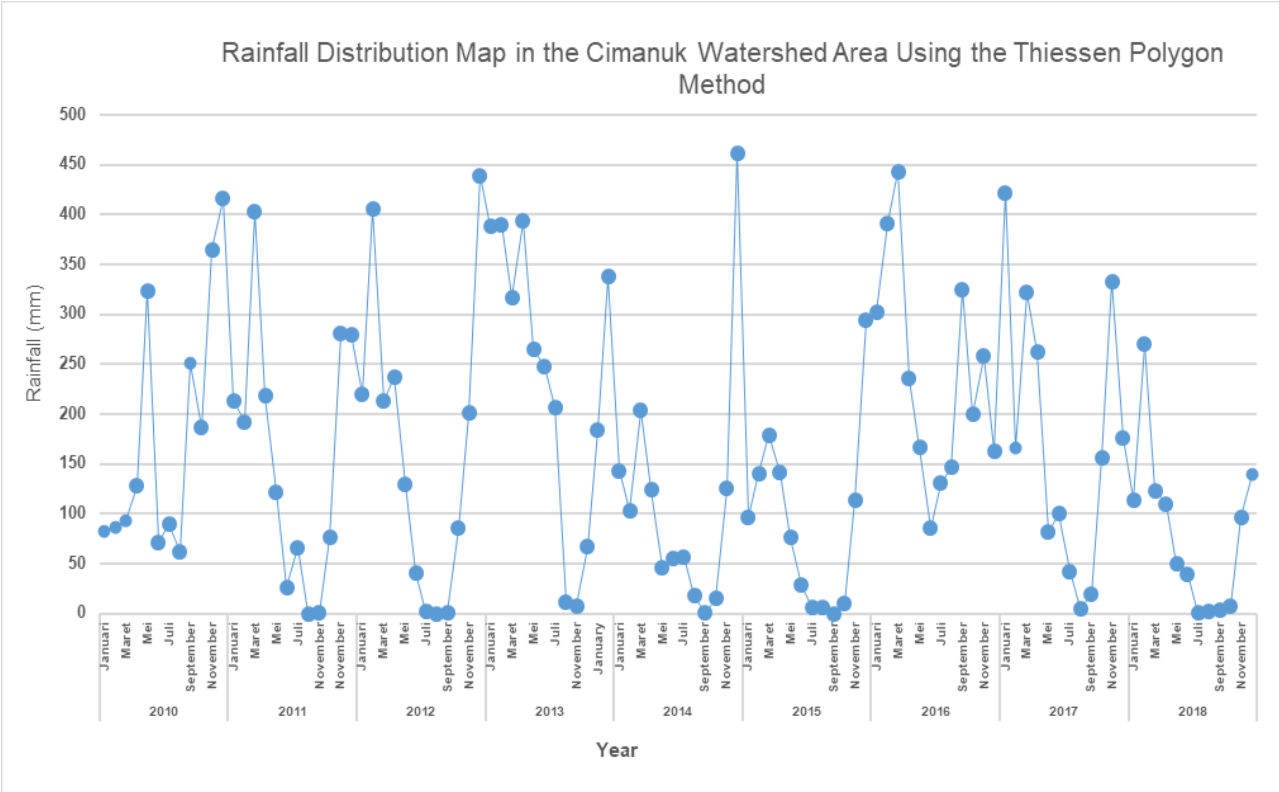

Figure 10. Monthly rainfall distribution over eight years in the Cimanuk Watershed using the Thiessen Polygon method

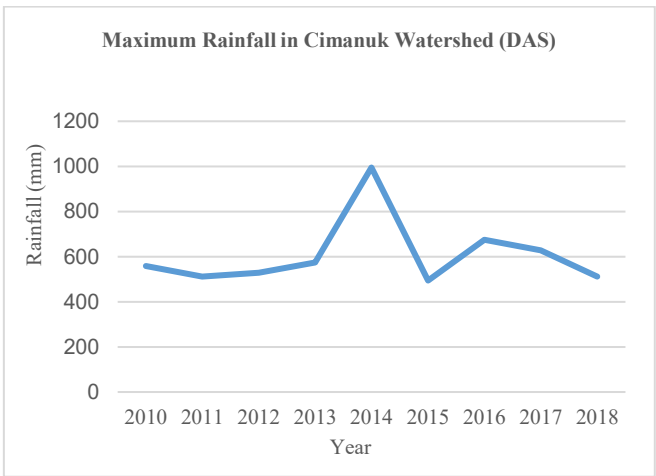

Figure 11. Maximum rainfall in the Cimanuk Watershed

To better understand the influence of topography on rainfall distribution, a statistical analysis was performed to examine the relationship between the elevation of rainfall stations and their corresponding annual average rainfall. Elevation data for the four stations were estimated based on DEM data and regional topography (See Table 11 and Figure 12).

Table 11. DEM data and regional topography

Station	Elevation (msl)	Average Annual Rainfall (2010-2018) (mm)	Standard Deviation of Annual Rainfall (mm)
Cikajang	1100	2240	210
Bayongbong	800	1900	180
Darmaraja	600	1550	150
Jatigede	200	1300	110

Figure 12 shows the correlation between elevation and rainfall across these stations. A Pearson correlation coefficient of $r = 0.97$ ($p < 0.05$) confirms a very strong positive relationship, suggesting that higher elevations consistently receive greater amounts of rainfall. This pattern supports the orographic effect, whereby moist air masses are forced to rise

over mountainous terrain, cool, and condense into precipitation. In addition to the annual relationship, monthly Pearson correlation values (see below) reinforce the consistency of this elevation-rainfall relationship throughout the year. The correlation values range from 0.60 (July) to 0.94 (December), indicating that orographic influence persists across seasons but is strongest during peak rainfall months.

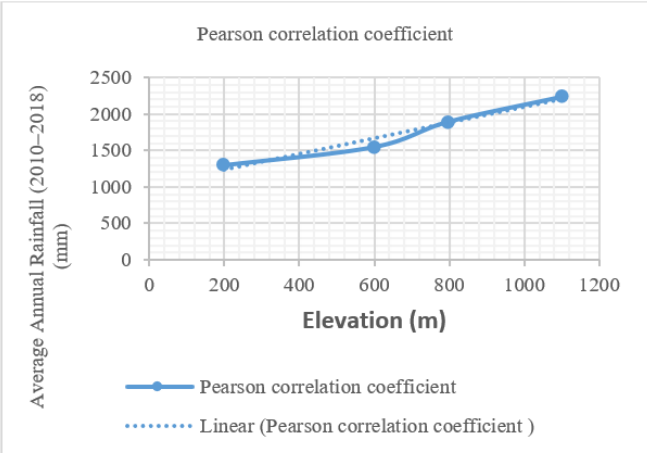

Figure 12. Maximum rainfall in the Cimanuk Watershed

Regression Equation

$$y = 1.0661x + 1027.89 \quad (6)$$

where, x = Elevation in meters (m); y = Average annual rainfall in millimeters (mm); r = 0.98 ($p < 0.05$), indicating a very strong and statistically significant positive correlation.

Every 100-meter increase in elevation is associated with an approximate 106.61mm increase in annual rainfall, confirming the strong orographic influence in the Cimanuk Watershed. The Pearson correlation between elevation and average annual rainfall was found to be r = 0.97 ($p < 0.01$), indicating a very strong positive relationship. Monthly temporal analysis revealed that the correlation varied throughout the year, with the lowest values occurring during the dry season (June to August), while remaining significantly positive during peak rainfall months (see Table 12).

Table 12. Elevation-Rainfall correlation by Month (2010-2018)

Month	Elevation-Rainfall Correlation (r)
January	0.85
February	0.87
March	0.89
April	0.91
May	0.93
June	0.62
July	0.60
August	0.65
September	0.88
October	0.90
November	0.92
December	0.94

Topographic Interpretation and Its Implications for Rainfall Distribution: Following the spatial rainfall distribution analysis presented in the previous subsection, a more detailed investigation was conducted to evaluate the influence of topography on rainfall variability within the Cimanuk Watershed. Understanding this relationship is essential for interpreting spatial heterogeneity in precipitation and for improving hydrological modeling accuracy. The analysis revealed that elevation plays a critical role in determining both the intensity and distribution of rainfall in the watershed. Orographic processes cause moist air masses to ascend mountainous terrain, where they cool and condense, leading to higher precipitation levels at higher elevations compared to lowland areas. This pattern is well-aligned with observed data from four primary rainfall stations—Cikajang (1100 m), Bayongbong (800 m), Darmaraja (600 m), and Jatigede (200 m). To quantify this relationship, a Pearson correlation analysis was performed between station elevation and corresponding average annual rainfall (2010–2018). The results showed a very strong positive correlation coefficient of r = 0.97 ($p < 0.05$), confirming that higher elevations tend to receive significantly greater rainfall. This supports the theoretical framework of orographic precipitation, as illustrated in Figure 12 and detailed in Table 11. In addition to annual analysis, monthly correlation values were also calculated to observe seasonal variation. These values—summarized in Table 12—show that correlation strength varies throughout the year. While the dry months (June to August) exhibit lower correlation (r = 0.60-0.65), the correlation becomes significantly stronger during peak rainy months, reaching up to r = 0.94 in December. This indicates that factors beyond topography, such as seasonal wind patterns and atmospheric dynamics, may have a greater influence on rainfall during the dry season, while topography dominates during wetter periods.

Rainfall Station and Streamflow Gauge Locations Analysis

To support rainfall distribution analysis within the Cimanuk Watershed, several rainfall monitoring stations have been established across different subregions. The placement of rainfall stations is essential in a watershed for understanding the rainfall distribution across the area [69, 70]. These stations are strategically positioned to capture precipitation data, which serve as critical inputs for hydrological modeling, runoff estimation, and flood risk assessment. Table 13 presents the geographical coordinates of four key rainfall stations currently operating in the watershed—Cikajang, Bayongbong, Darmaraja, and Jatigede—each located at varying elevations and spatial zones within the catchment. Their placement aims to represent spatial rainfall variation influenced by topographic and climatic factors.

Table 13. Rainfall station locations in the Cimanuk Watershed

No.	Watershed	Station Name	Coordinates (Y, X)	
			Y	X
1	Cimanuk	Cikajang	-7.3464	107.8015
2	Cimanuk	Bayongbong	-7.2724	107.8168
3	Cimanuk	Darmaraja	-6.9138	10807495
4	Cimanuk	Jatigede	-6.8569	108.1082

However, the current rainfall station network in the Cimanuk Watershed is insufficient to adequately capture the spatial variability of rainfall, particularly given the watershed's pronounced topographic complexity. The limited number and uneven distribution of stations hinder the ability to represent microclimatic differences, especially in highland

areas where orographic effects significantly influence precipitation patterns. Increasing the density of rainfall stations—especially in higher elevation zones—is therefore critical to improve the accuracy of spatial rainfall interpolation, enhance hydrological model performance, and support more reliable flood forecasting. A denser and strategically distributed station network would allow for better resolution of rainfall gradients across elevation bands, ultimately providing more robust data inputs for watershed-scale hydrological analysis and disaster risk reduction planning. Figure 13 illustrates the insufficient rainfall station network in the Cimanuk Watershed to capture rainfall variability, given its complex topography.

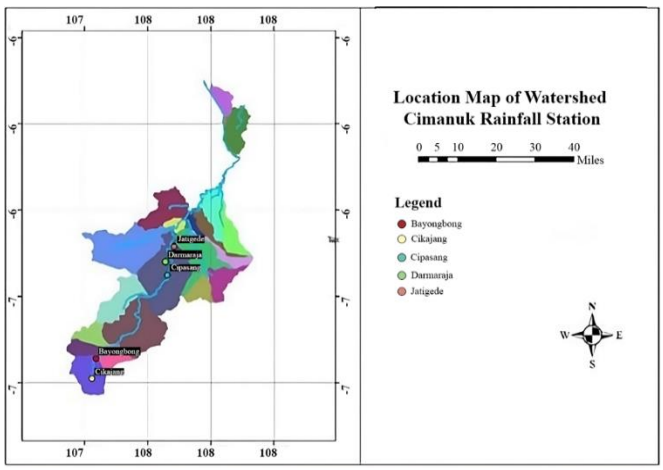

Figure 13. Map of rainfall station locations in the Cimanuk Watershed

Table 14. Coverage area of the Cimanuk watershed using the Thiessen Polygon method

Station	Coverage Area (Ha)
Cikajang	4922.16
Bayongbong	58902.8
Darmaraja	81581.9
Jatigede	5358.51
Total	150765.37

Table 15. Coverage area of Cimanuk Watershed using the Kriging method

No.	Classification (%)	Area (Ha)
1	33.2-35	1089.52
2	35-45	25877.3
3	45-55	33419.6
4	55-65	24119.2
5	65-90	47590.5
	Total	132096.12

The Cimanuk Watershed is also equipped with several streamflow gauges (see Table 14), each contributing to the analysis of the surrounding regions. Topographic complexity requires a denser station network to accurately capture rainfall variability, particularly across elevation gradients. This is essential for improving hydrological model inputs and flood forecasting accuracy.

Distribution Pattern Analysis Using the Thiessen Polygon Method

Once the rainfall station coordinates within the Cimanuk Watershed are known, the extent of the coverage areas of these rainfall stations (see Table 15) and streamflow gauges can be analyzed using the Thiessen Polygon method with GIS software. The results provide a map indicating the distribution of the coverage areas. The results are presented in Figure 14, which shows a map indicating the distribution of the coverage areas.

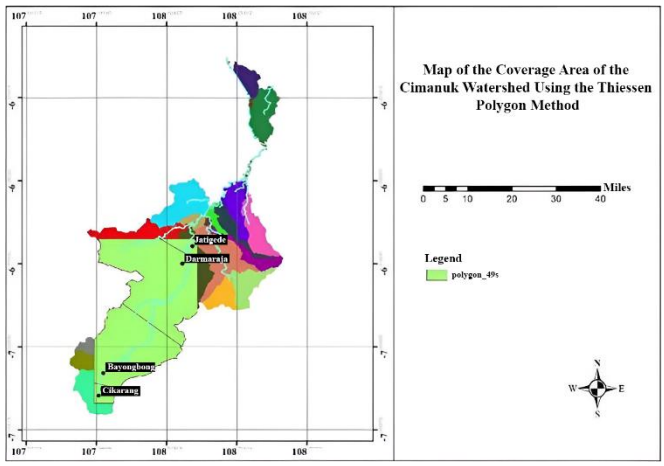

Figure 14. Coverage area map of the Cimanuk Watershed using the Thiessen Polygon method

The spatial pattern of rainfall coverage highlights the influence of topography, with higher-elevation stations capturing larger orographic zones. This underscores the importance of incorporating elevation into rainfall interpolation and hydrological analysis to reduce estimation uncertainty, particularly in mountainous regions.

Ecohydrological Significance of CT Values: The Thiessen Constant (CT) values derived from the Thiessen Polygon method represent the proportional area coverage each rainfall station influences in the watershed. From an ecohydrological perspective, these CT values are more than just mathematical weights—they reflect spatial zones where rainfall input is critical for hydrological processes and ecosystem dynamics. Areas with high CT values exert greater influence on the watershed's hydrological response, particularly in generating surface runoff and recharging groundwater. These regions are often hotspots for controlling streamflow variability and sustaining aquatic and riparian ecosystems. Moreover, the ecohydrological significance extends to understanding watershed vulnerability. Changes in land use or vegetation cover within high-CT areas can disproportionately alter hydrological patterns, increasing erosion risk, sediment load, and flood potential downstream. Therefore, mapping and analyzing CT values aid in prioritizing conservation efforts and water resource management, ensuring that interventions target regions where rainfall inputs have the most substantial hydrological and ecological impact.

Distribution Pattern Analysis Using the Kriging Method

The distribution pattern can also be analyzed using the Kriging method [71] after determining the coordinates of rainfall stations within the Cimanuk Watershed. The Kriging method offers a more refined interpolation of the affected regions based on the available rainfall data (see Table 16).

Results from Kriging further confirm that rainfall distribution is heterogeneous and closely linked to terrain features, reinforcing the necessity to consider topographic variables in hydrological assessments.

Ecohydrological Implications of Kriging-Based Rainfall Distribution: The Kriging interpolation method generates a continuous and spatially detailed rainfall surface that effectively captures the complex variability of precipitation across the Cimanuk Watershed, especially in areas with significant topographic variation. This spatial refinement allows for a more precise understanding of how rainfall patterns influence hydrological processes such as surface runoff, infiltration, and groundwater recharge (see Figure 15). From an ecohydrological perspective, the detailed rainfall distribution produced by Kriging supports better identification of critical zones within the watershed where water availability and flow regimes directly affect ecosystem health and function. Consequently, using Kriging enhances the capacity to design targeted watershed management and conservation strategies by highlighting spatial heterogeneity in rainfall inputs that drive ecological and hydrological responses.

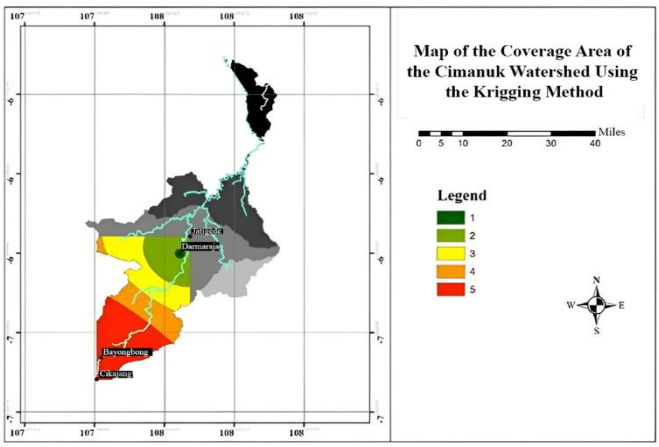

Figure 15. Coverage area map of the Cimanuk Watershed using the Thiessen Polygon method

Table 16. Comparison between Thiessen and Kriging methods

Method	Total Area (Ha)	Notes
Thiessen	150,765.37	Piecewise constant, abrupt boundaries, fast
Kriging	132,096.12	Smooth surface, incorporates spatial autocorrelation

Comparison Between Thiessen and Kriging Methods

This study employed both the Thiessen Polygon and Kriging methods to interpolate rainfall distribution across the Cimanuk Watershed using data from four rainfall stations over 2010-2018. The Thiessen method yielded coverage areas for each station (Table 14), generating a piecewise constant rainfall distribution where rainfall values are uniform within each polygon. This method is simple and computationally efficient but results in abrupt boundaries and does not account for spatial correlation between stations. Conversely, the Kriging method produced a smoother rainfall distribution (Table 15) that incorporates spatial autocorrelation, better capturing gradual changes in rainfall intensity across the watershed. The classification of rainfall percentages by area from Kriging shows differences compared to Thiessen, for example: Kriging class 65–90% rainfall covers 47,590.5 ha, while Thiessen assigns this rainfall intensity differently. These differences indicate that Kriging provides a more realistic representation of rainfall variability, especially in areas with complex topography and sparse station data. However, Kriging requires more detailed data and computational resources, while Thiessen remains valuable for rapid estimation and when data are limited. In hydrological modeling applications, especially in complex terrain like Cimanuk, the Kriging method is preferable to reduce interpolation errors and better inform water resource management decisions.

CN Value Analysis in the Cimanuk Watershed

The CN value analysis for the Cimanuk Watershed was conducted using the SCS method, which incorporates land use, land cover, and sub-watershed data. The CN values were derived by overlaying the land use and soil maps, with soil types classified into HSGs A–D based on NRCS (TR-55) criteria. The combination of these classes under normal moisture conditions yielded CN values following the standard lookup tables. Each land cover type was matched with its corresponding CN value based on its hydrologic group, allowing accurate estimation of surface runoff potential across the sub-watersheds. The results of the CN analysis are presented in Table 17.

From Table 17, it can be concluded that the average CN value for the Cimanuk Watershed is 61.472, calculated using the SCS-CN method. The average CN value for the watershed was calculated to be 61.472, representing moderate runoff potential. This value was used in surface runoff estimations. The method aligns with best practices in recent literature [26, 27] for tropical watersheds with complex terrain and limited data.

Table 17. CN value of Cimanuk Watershed

No.	Land Cover Type	Area (ha)	%	Soil Group					
				A		B		C	
				CN	Value	CN	Value	CN	Value
1	Primary Dry Forest	2968	0.9	45	41				
2	Secondary Dry Forest	12002	3.7	45	165				
3	Plantations	57820	17.7	25	442				
4	Plantation Crops	3776	1.2			71	82		
5	Residential Areas	26918	8.2	77	633				
6	Dryland Agriculture	80524	24.6	68	1672				
7	Dryland Agriculture + Scrub	38436	11.7	68	798				
8	Rice Fields	95667	29.2			71	2075		
9	Scrubland/Thickets	1762	0.5	45	24				
10	Salt Ponds	4280	1.3			98	128		
11	Bare Land	1704	0.5					79	41
12	Water Bodies	1541	0.5					98	46
	Total Area (Ha)	327399	100		3775		2285		87
	CN Value						61.472		

Table 18. Rainfall-Runoff relationship

Year	Cikajang (mm)	Bayongbong (mm)	Darmaraja (mm)	Jatigede (mm)	Runoff Discharge (m³/s)
2010	2200	1900	1500	1300	18.5
2011	2100	1850	1480	1250	17.8
2012	2300	1950	1550	1350	19.2
2013	2400	2000	1600	1400	20.0
2014	2500	2100	1650	1450	20.8
2015	2150	1875	1500	1300	18.0
2016	2250	1920	1555	1330	19.0
2017	2350	1980	1580	1380	19.8
2018	2200	1900	1520	1320	18.7

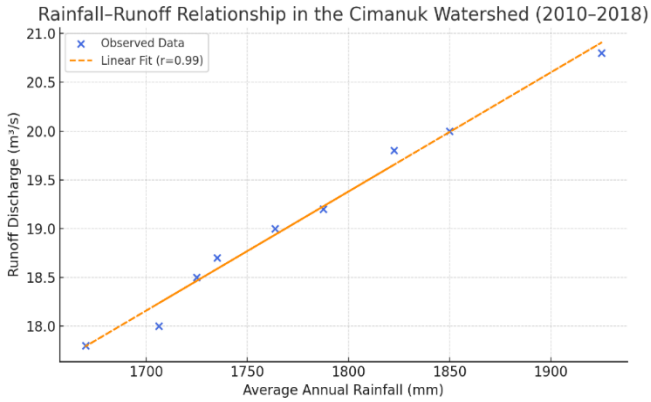

Figure 16. Rainfall-Runoff relationship

Rainfall-Runoff relationship

This section explains the direct relationship between precipitation and runoff, which contributes to flood risk and hydrological changes within the watershed (see Table 18 and Figure 16). The diagram reinforces the results of the SCS-CN model and supports recommendations for integrated water resource management.

Rainfall-Runoff Relationship Equation

$$y = 0.0061x + 4.72 \quad (7)$$

where, x = Average annual rainfall in millimeters (mm), computed as the mean of four stations: Cikajang, Bayongbong, Darmaraja, and Jatigede; y = Runoff discharge in cubic meters per second (m³/s).

Rainfall-Runoff Relationship (See Figure 16): The scatter plot above illustrates the relationship between average annual rainfall (from four stations: Cikajang, Bayongbong, Darmaraja, and Jatigede) and streamflow discharge. A strong positive linear correlation was found, with: (1) Pearson correlation coefficient: r = 0.99; (2) Significance level: $p < 0.001$. This confirms that rainfall is the dominant driver of surface runoff in the watershed. The trendline reinforces the assumption that as average annual rainfall increases, runoff discharge rises proportionally, validating the use of the SCS-CN model for runoff estimation in this region. Moreover, the observed scatter reflects secondary influences such as: Land cover variations (e.g., agricultural dominance in lower zones), Soil infiltration characteristics, Temporal rainfall distribution (seasonality).

Analysis of the Rationality of Rainfall Station Density in the Cimanuk Watershed

In analyzing the rainfall density, data on the area size and topographic characteristics of the Cimanuk Watershed were used. Based on its topographic conditions, the Cimanuk Watershed falls under type 2: Tropical Mediterranean and Moderate Mountainous Areas, as shown in Table 2 about Network density according to WMO. The conditions in the Cimanuk Watershed fall under the normal category. Based on the area of the Cimanuk Watershed, which is 327,399.4 ha, when converted to km², it becomes 3,273.99 km² (see Table 19). With the topographic conditions of the Cimanuk Watershed being a tropical Mediterranean and moderate mountainous area in normal conditions, the result is an area of 100–250 km² per rainfall station.

Table 19. Network density analysis

Description	Area (Km²)	Number of Stations
As Built	3273,99	6
According to WMO		13

Rainfall Station Density and Topographic Influence: Rainfall distribution in the Cimanuk Watershed is strongly influenced by topography (see Table 19), with higher elevations receiving significantly more precipitation due to orographic effects. This variability is especially pronounced in the upper catchment areas, such as Garut and Bayongbong. However, the current network of only 6 rainfall stations is insufficient to capture this spatial heterogeneity. Based on WMO guidelines—which recommend 1 station per 100 - 250 km² in mountainous terrain—the Cimanuk Watershed requires at least 13 stations. The limited number of stations, particularly in high-altitude zones, may lead to inaccuracies in rainfall interpolation, runoff estimation (e.g., SCS-CN modeling), and flood risk assessment. Improving station density, especially across elevation gradients, is essential for enhancing hydrological modeling, flood forecasting, and integrated watershed management. Furthermore, the strong correlation between elevation and rainfall intensity (r = 0.97) highlights the need to incorporate topographic data into modeling frameworks. In conclusion, the watershed's complex terrain, diverse land use (with ~25% dryland agriculture), and erosion-prone slopes necessitate a more robust monitoring system. Expanding the station network and integrating elevation-based analysis will improve climate resilience strategies and ensure more effective and data-driven water resource management.

3.2 Discussion

This study underscores the critical role of spatial rainfall variability and its interaction with watershed characteristics in determining hydrological responses in the Cimanuk Watershed. The ecohydrological interpretation of Thiessen Constants highlights spatial heterogeneity in rainfall influence, guiding focused management in areas with the greatest hydrological sensitivity. The comparison of Thiessen

and Kriging interpolation methods further clarifies the trade-offs between computational simplicity and spatial accuracy, with Kriging offering more nuanced rainfall surfaces better suited for modeling in complex terrains. The integration of Curve Number analysis with spatial rainfall patterns and CT values provides a comprehensive framework for understanding runoff generation mechanisms. Given the identified insufficient density of rainfall stations, especially in high-CT zones, there is a strong imperative to expand the monitoring network to capture spatial rainfall dynamics accurately. This will improve model calibration, enhance flood prediction, and support effective land and water resource management. Additionally, land use changes within the watershed, particularly in areas of high hydrological sensitivity indicated by CT, necessitate careful planning to mitigate adverse ecological and hydrological impacts.

4. CONCLUSION

This study provides a comprehensive analysis of the Cimanuk Watershed's hydrological behavior by integrating spatial rainfall distribution, land use, soil types, and topographic variation across its 3,600 km² area. The strong positive correlation between elevation and rainfall ($r = 0.97$, $p < 0.05$) confirms the dominant role of orographic effects, particularly in upper catchments like Garut and Bayongbong. Seasonal and interannual variability—peaking in 2017 and lowest in 2018—further underscores the importance of continuous rainfall monitoring. Using GIS, two interpolation methods were compared: Thiessen Polygon and Kriging. Kriging produced more spatially detailed outputs, while Thiessen yielded broader, average-based zones. Thiessen Constants (CT values) not only serve as spatial weights but also as ecohydrological indicators, highlighting zones with disproportionate hydrological influence.

The SCS-CN model produced an average Curve Number of 61.472, indicating moderate runoff potential influenced by the basin's dominant agricultural land uses and soil types. This value is crucial for flood forecasting and water resource planning. Despite the watershed's complexity, only 6 rain gauge stations are currently operational—less than half of the 13 recommended by WMO standards. This sparse network limits the spatial representativeness of rainfall data, increasing uncertainty in hydrological modeling and risk assessments.

GIS analyses revealed severe coverage gaps, especially in high-relief and ecologically sensitive areas. Strengthening the rainfall monitoring network—particularly across elevation gradients—is essential for improving data accuracy, flood risk forecasting, and long-term watershed management.

In conclusion, rainfall distribution significantly shapes hydrological responses in the Cimanuk Watershed. This study demonstrates the critical role of GIS in evaluating network adequacy and supports strategic station expansion to enhance modeling reliability and resilience planning. By identifying high-impact areas through CT and runoff analyses, the findings inform targeted interventions for flood mitigation, conservation prioritization, and sustainable water resource management.

ACKNOWLEDGMENT

The study was self-funded, BRIN Indonesia (Badan Riset and Innovation National, Indonesia) and Universitas Pancasila for providing office.

REFERENCES

[1] Naiman, R.J., Bisson, P.A., Lee, R.G., Turner, M.G. (1998). Watershed management. In River Ecology and Management: Lessons from The Pacific Coastal Ecoregion. Springer-Verlag, New York, pp. 642-661.

[2] Plamonia, N. (2010). Kajian Pengaruh Kenaikan Muka Air Laut, Reklamasi Pantai dan Degradasi Lahan di DAS Hulu Terhadap Banjir di pesisir Terbangun DKI Jakarta–DAS Ciliwung. Master Thesis. Institut Teknologi Bandung.

[3] Ariyani, D., Purwanto, M.Y.J., Sunarti, E., Perdinan, Arini, R.N., Phratama, S., Ibrahim, M. (2024). Comparison of the Nakayasu, gamma, and Snyder hydrograph model to determining flood water level for the early warning system in the Ciliwung River. AIP Conference Proceedings, 2838(1): 040002. https://doi.org/10.1063/5.0179732

[4] Thiessen, A.H. (1911). Precipitation averages for large areas. Monthly Weather Review, 39(7): 1082-1089. https://doi.org/10.1175/1520-0493(1911)39%3C1082b:PAFLA%3E2.0.CO;2

[5] Olawoyin, R., Acheampong, P.K. (2017). Objective assessment of the Thiessen polygon method for estimating areal rainfall depths in the River Volta catchment in Ghana. Ghana Journal of Geography, 9(2): 151-174.

[6] Taesombat, W., Sriwongsitanon, N. (2009). Areal rainfall estimation using spatial interpolation techniques. Science Asia, 35(3): 268-275.

[7] Zhang, X., Srinivasan, R. (2009). GIS-based spatial precipitation estimation: A comparison of geostatistical approaches 1. JAWRA Journal of The American Water Resources Association, 45(4): 894-906. https://doi.org/10.1111/j.1752-1688.2009.00335.x

[8] Trirahadi, A., Bafdal, N., Amaru, K., Ridwansyah, I. (2022). Perubahan tata guna lahan terhadap limpasan permukaan di sub DAS cimanuk hulu menggunakan model soil and water assesment tool (SWAT). In Seminar Nasional Lppm Ummat, 1: 599-615.

[9] Kaliraj, S., Chandrasekar, N., Ramachandran, K.K., Lalitha, M. (2023). GIS based NRCS-CN modeling of rainfall-runoff in river Thamirabarani sub-basin, Southern India. Journal of Hydro-Environment Research, 49: 10-27. https://doi.org/10.1016/j.jher.2023.07.001

[10] Juniati, A.T., Plamonia, N., Ariyani, D., Fitrah, M., Kuncoro, D.A. (2025). Landslide hazard mapping and bio-engineering solutions for riverbank stabilization in the Cisanggarung River Basin, Indonesia: A GIS-based approach. Journal of Degraded and Mining Lands Management, 12(3): 7637-7648. https://doi.org/10.15243/jdmlm.2025.123.7637

[11] Kumar, A., Kanga, S., Taloor, A.K., Singh, S.K., Đurin, B. (2021). Surface runoff estimation of Sind River Basin using integrated SCS-CN and GIS techniques. HydroResearch, 4: 61-74. https://doi.org/10.1016/j.hydres.2021.08.001

[12] Pandey, P., Tiwari, S.K., Pandey, H.K., Chaurasia, A.K., Singh, S. (2021). Identification of potential recharge

zones in drought prone area of Bundelkhand region, India, using SCS-CN and MIF technique under GIS-frame work. Water Conservation Science and Engineering, 6(3): 105-125. https://doi.org/10.1007/s41101-021-00105-0

[13] Dong, Z., Bain, D.J., Akcakaya, M., Ng, C.A. (2023). Evaluating the Thiessen polygon approach for efficient parameterization of urban stormwater models. Environmental Science and Pollution Research, 30(11): 30295-30307. https://doi.org/10.1007/s11356-022-24162-7

[14] Zhang, G., Tian, G., Cai, D., Bai, R., Tong, J. (2021). Merging radar and rain gauge data by using spatial–temporal local weighted linear regression kriging for quantitative precipitation estimation. Journal of Hydrology, 601: 126612. https://doi.org/10.1016/j.jhydrol.2021.126612

[15] William, K.H., Hutomo, K.D. (2021). The natural disaster prone index map model in indonesia using the thiessen polygon method. INTENSIF: Jurnal Ilmiah Penelitian dan Penerapan Teknologi Sistem Informasi, 5(2): 148-160. https://doi.org/10.29407/intensif.v5i2.14612

[16] Jayanti, M., Sabar, A., Ariesyady, H.D., Marselina, M., Qadafi, M. (2023). A comparison of three water discharge forecasting models for monsoon climate region: A case study in cimanuk-jatigede watershed Indonesia. Water Cycle, 4: 17-25. https://doi.org/10.1016/j.watcyc.2023.01.002

[17] Das, S., Islam, A.R.M.T. (2021). Assessment of mapping of annual average rainfall in a tropical country like Bangladesh: Remotely sensed output vs. kriging estimate. Theoretical and Applied Climatology, 146(1): 111-123. https://doi.org/10.1007/s00704-021-03729-3

[18] Jayanti, M., Marganingrum, D., Plamonia, N., Santoso, H., Marselina, M., Ariesyady, H.D., Sabar, A. (2025). The operation optimization of multipurpose reservoir between ARIMA, continuous, and Markov Chain models on Jatigede reservoir, Indonesia. Water Cycle, 6: 399-411.

[19] Ben-Daoud, M., El Mahrad, B., Elhassnaoui, I., Moumen, A., Sayad, A., ELbouhadioui, M., Moroșanu, G.A., Mezouary, L.E., Essahlaoui, A., Eljaafari, S. (2021). Integrated water resources management: An indicator framework for water management system assessment in the R'Dom Sub-basin, Morocco. Environmental Challenges, 3: 100062. https://doi.org/10.1016/j.envc.2021.100062

[20] Lemaire, G.G., Rasmussen, J.J., Höss, S., Kramer, S.F., Schittich, A.R., Zhou, Y., Köppl, C.J., Traunspurger, W., Bjerg, P.L., McKnight, U.S. (2022). Land use contribution to spatiotemporal stream water and ecological quality: Implications for water resources management in peri-urban catchments. Ecological Indicators, 143: 109360. https://doi.org/10.1016/j.ecolind.2022.109360

[21] Bilalova, S., Newig, J., Tremblay-Lévesque, L.C., Roux, J., Herron, C., Crane, S. (2023). Pathways to water sustainability? A global study assessing the benefits of integrated water resources management. Journal of Environmental Management, 343: 118179.

[22] Maranzoni, A., D'Oria, M., Rizzo, C. (2023). Quantitative flood hazard assessment methods: A review. Journal of Flood Risk Management, 16(1): e12855. https://doi.org/10.1111/jfr3.12855

[23] Plamonia, N., Putra, A.P., Yunus, A.F., Saptiarini, D., Lesman, S., Bukit, D.L., Wijayanti, S., A, D.N., Widyastuti, I. (2025). Comparative analysis of multi-utility tunnel and conventional methods: Evaluating cost efficiency, soil stability, and sustainability for infrastructure development in IKN, Nusantara. Mathematical Modelling of Engineering Problems, 12(6): 1981-1996. https://doi.org/10.18280/mmep.120614

[24] Merino, A., García-Ortega, E., Navarro, A., Fernández-González, S., Tapiador, F.J., Sánchez, J.L. (2021). Evaluation of gridded rain-gauge-based precipitation datasets: Impact of station density, spatial resolution, altitude gradient and climate. International Journal of Climatology, 41(5): 3027-3043. https://doi.org/10.1002/joc.7003

[25] Suri, A., Azad, S. (2024). Optimal placement of rain gauge networks in complex terrains for monitoring extreme rainfall events: A review. Theoretical and Applied Climatology, 155(4): 2511-2521. https://doi.org/10.1007/s00704-024-04856-3

[26] Kara, B., Baykurt, G. (2022). Using the SCS curve number method for rainwater harvesting: A case study from Yenipazar, Turkey. International Journal of Advances in Engineering and Management, 4(4): 1204-1216.

[27] Eniyew, S., Meshesha, D.T., Zeleke, G.A., Wassie, S.B. (2024). Combining geospatial information and SCS-CN for surface runoff estimation in Rib watershed, upper Blue Nile Basin, Ethiopia. Geomatics, Natural Hazards and Risk, 15(1): 2338533. https://doi.org/10.1080/19475705.2024.2338533

[28] Taye, G., Vanmaercke, M., van Wesemael, B., Tesfaye, S., Teka, D., Nyssen, J., Deckers, J., Poesen, J. (2023). Estimating the runoff response from hillslopes treated with soil and water conservation structures in the semi-arid Ethiopian highlands: Is the curve number method applicable?. Scientific African, 20: e01620. https://doi.org/10.1016/j.sciaf.2023.e01620

[29] Pishvaei, M.H., Noroozpour, S., Sabzevari, T., Kheirabadi, M.A., Petroselli, A. (2024). Spatial and temporal distribution of infiltration, curve number and runoff coefficients using TOPMODEL and SCS-CN models. Journal of Agriculture and Environment for International Development (JAEID), 118(2): 203-230. https://doi.org/10.36253/jaeid-15317

[30] Akhtar, F., Awan, U.K., Borgemeister, C., Tischbein, B. (2021). Coupling remote sensing and hydrological model for evaluating the impacts of climate change on streamflow in data-scarce environment. Sustainability, 13(24): 14025. https://doi.org/10.3390/su132414025

[31] Shaikh, M., Birajdar, F. (2024). Advancements in remote sensing and GIS for sustainable groundwater monitoring: Applications, challenges, and future directions. International Journal of Research in Engineering, Science and Management, 7(3): 16-24.

[32] Azizah, A., Welastika, R., Falah, A.N., Ruchjana, B.N., Abdullah, A.S. (2019). An application of Markov chain for predicting rainfall data at West Java using data mining approach. IOP Conference Series: Earth and Environmental Science, 303(1): 012026. https://doi.org/10.1088/1755-1315/303/1/012026

[33] Trinugroho, M.W., Nguyen, D.H. (2021). Assessing

freshwater water balance in Cimanuk River Basin. IOP Conference Series: Earth and Environmental Science, 648(1): 012094. https://doi.org/10.1088/1755-1315/648/1/012094
[34] Rusydi, A.F., Onodera, S.I., Saito, M., Ioka, S., Maria, R., Ridwansyah, I., Delinom, R.M. (2021). Vulnerability of groundwater to iron and manganese contamination in the coastal alluvial plain of a developing Indonesian city. SN Applied Sciences, 3(4): 399. https://doi.org/10.1007/s42452-021-04385-y
[35] Ismail, A.Y., Aminudin, S., Andayani, S.A., Sumekar, Y. (2021). Analysis of land use patterns in the upper Cimanuk river basin and its relationship with irrigation water discharge in Majalengka Regency, Indonesia. Research on Crops, 22(4): 836-840.
[36] Yuanita, N., Tingsanchali, T. (2008). Development of a river delta: A case study of Cimanuk river mouth, Indonesia. Hydrological Processes: An International Journal, 22(18): 3785-3801. https://doi.org/10.1002/hyp.6987
[37] Sidel, J.L., Bleibaum, R.N., Tao, K.C. (2018). Quantitative descriptive analysis. In Descriptive Analysis in Sensory Evaluation, pp. 287-318. https://doi.org/10.1002/9781118991657.ch8
[38] Siedlecki, S.L. (2020). Understanding descriptive research designs and methods. Clinical Nurse Specialist, 34(1): 8-12. https://doi.org/10.1097/NUR.0000000000000493
[39] Hodge, S.R. (2020). Quantitative research. In Routledge Handbook of Adapted Physical Education, Routledge, pp. 147-162.
[40] Plamonia, N., Dewa, R.P., Jayanti, M., Riyadi, A., Rahayu, B., Diyono, Sahwan, F.L., Chandra, H., Sulistiawan, I.N., Sudiana, N., Hidayat, N., Prasetiyadi, Tilottama, R.D., Irawanto, R., Wahyono, S., Suprapto, Juniati, A.T., Prasidha, I.N.T. (2025). Sustainable water distribution design for Indonesia's new capital, Nusantara: Integrating eco-design and economic principles. International Journal of Sustainable Development and Planning, 20(2): 537-554. https://doi.org/10.18280/ijsdp.200207
[41] Wolock, D.M., Price, C.V. (1994). Effects of digital elevation model map scale and data resolution on a topography-based watershed model. Water Resources Research, 30(11): 3041-3052. https://doi.org/10.1029/94WR01971
[42] Plamonia, N., Anjani, R., Amru, K., Sudaryanto, A. (2024). Exploring effective institutional models for piped drinking water management: A comparative study of Jakarta and Kuala Lumpur and proposal of a new model for Indonesia's new capital city. Water Practice & Technology, 19(12): 4734-4753. https://doi.org/10.2166/wpt.2024.291
[43] Öztürk, M., Copty, N.K., Saysel, A.K. (2013). Modeling the impact of land use change on the hydrology of a rural watershed. Journal of Hydrology, 497: 97-109. https://doi.org/10.1016/j.jhydrol.2013.05.022
[44] Horton, R.E. (1939). Analysis of runoff-plat experiments with varying infiltration-capacity. Eos, Transactions American Geophysical Union, 20(4): 693-711. https://doi.org/10.1029/TR020i004p00693
[45] Fernandez, C., Wu, J.Q., McCool, D.K., Stöckle, C.O. (2003). Estimating water erosion and sediment yield with GIS, RUSLE, and SEDD. Journal of Soil and Water Conservation, 58(3): 128-136. https://doi.org/10.1080/00224561.2003.12457515
[46] Belayneh, M., Yirgu, T., Tsegaye, D. (2019). Potential soil erosion estimation and area prioritization for better conservation planning in Gumara watershed using RUSLE and GIS techniques'. Environmental Systems Research, 8(1): 1-17. https://doi.org/10.1186/s40068-019-0149-x
[47] Jain, S.K., Kumar, S., Varghese, J. (2001). Estimation of soil erosion for a Himalayan watershed using GIS technique. Water Resources Management, 15: 41-54. https://doi.org/10.1023/A:1012246029263
[48] Gelagay, H.S., Minale, A.S. (2016). Soil loss estimation using GIS and Remote sensing techniques: A case of Koga watershed, Northwestern Ethiopia. International Soil and Water Conservation Research, 4(2): 126-136. https://doi.org/10.1016/j.iswcr.2016.01.002
[49] Koga, K., Araki, H., Liengcharernsit, W. (2022). Hydrological and environmental characteristics. In Lowlands. Routledge, pp. 41-63.
[50] Rijal, S., Samsuri, Masruroh, H., Nursaputra, M., Ardi, N.Z.P. (2025). Ecological sensitivity of the mata allo sub-watershed, south sulawesi: A spatial analysis using principal component analysis. Sustainability, 17(2): 447. https://doi.org/10.3390/su17020447
[51] Bronick, C.J., Lal, R. (2005). Soil structure and management: A review. Geoderma, 124(1-2): 3-22. https://doi.org/10.1016/j.geoderma.2004.03.005
[52] Wang, S., Adhikari, K., Wang, Q., Jin, X., Li, H. (2018). Role of environmental variables in the spatial distribution of soil carbon (C), nitrogen (N), and C: N ratio from the northeastern coastal agroecosystems in China. Ecological Indicators, 84: 263-272. https://doi.org/10.1016/j.ecolind.2017.08.046
[53] Haghverdi, K., Kooch, Y. (2020). Soil carbon and nitrogen fractions in response to land use/cover changes. Acta Oecologica, 109: 103659. https://doi.org/10.1016/j.actao.2020.103659
[54] NRCS, U. (1986). Urban hydrology for small watersheds-technical release 55. US Department of Agriculture Natural Resources Conservation: Washington, DC, USA.
[55] Usda, S. (1986). Urban hydrology for small watersheds. Technical Release, 55: 2-6.
[56] Plamonia, N., Saputra, E.R.A., Said, N.I., Hernaningsih, T., Widayat, W., Hanif, M., Adi, P.D., Yohanitas, W.A., Niode, N., Dewa, R.P., Witama, R.O. (2024). Penstock pipe's hydraulic design for the mini hydropower plant at Besai Kemu, Bukit Kemuning, Lampung, Indonesia. IOP Conference Series: Earth and Environmental Science, 1388(1): 012057. https://doi.org/10.1088/1755-1315/1388/1/012057
[57] Plamonia, N. I.C.C.O. (2020). Improving the coverage area of drinking water provision by using build operate and transfer investments in Indonesia. An Institutional Analysis. [Dissertation]. University of Twente. https://doi.org/10.3990/1.9789036550901
[58] Alemayehu, F., Taha, N., Nyssen, J., Girma, A., Zenebe, A., Behailu, M., Deckers, S., Poesen, J. (2009). The impacts of watershed management on land use and land cover dynamics in Eastern Tigray (Ethiopia). Resources, Conservation and Recycling, 53(4): 192-198. https://doi.org/10.1016/j.resconrec.2008.11.007
[59] Sajikumar, N., Remya, R.S. (2015). Impact of land cover

and land use change on runoff characteristics. Journal of Environmental Management, 161: 460-468. https://doi.org/10.1016/j.jenvman.2014.12.041
[60] Ismail, A.Y., Aminudin, S., Andayani, S.A., Sumekar, Y. (2021). Analysis of land use patterns in the upper Cimanuk river basin and its relationship with irrigation water discharge in Majalengka Regency, Indonesia. Research on Crops, 22(4): 836-840.
[61] van Tilburg, R. (2018). Hydrological and climate risk assessment for the Cimanuk River Basin, Indonesia. FutureWater Internship Report.
[62] Hatmoko, W., Firmansyah, R., Fathony, A. (2020). Water security of river basins in West Java. IOP Conference Series: Earth and Environmental Science, 419(1): 012140. https://doi.org/10.1088/1755-1315/419/1/012140
[63] Haregeweyn, N., Tsunekawa, A., Poesen, J., Tsubo, M., Meshesha, D.T., Fenta, A.A., Nyssen, J., Adgo, E. (2017). Comprehensive assessment of soil erosion risk for better land use planning in river basins: Case study of the Upper Blue Nile River. Science of The Total Environment, 574: 95-108. https://doi.org/10.1016/j.scitotenv.2016.09.019
[64] Altaf, S., Meraj, G., Romshoo, S.A. (2014). Morphometry and land cover based multi-criteria analysis for assessing the soil erosion susceptibility of the western Himalayan watershed. Environmental Monitoring and Assessment, 186: 8391-8412. https://doi.org/10.1007/s10661-014-4012-2
[65] Bilaşco, Ş., Roşca, S., Păcurar, I., Moldovan, N., Boţ, A., NegruȘIER, C., Sestras, P., Bondrea, M. NaȘ, S. (2016). Identification of land suitability for agricultural use by applying morphometric and risk parameters based on GIS spatial analysis. Notulae Botanicae Horti Agrobotanici Cluj-Napoca, 44(1): 302-312. https://doi.org/10.15835/nbha44110289
[66] Akıncı, H., Özalp, A.Y., Turgut, B. (2013). Agricultural land use suitability analysis using GIS and AHP technique. Computers and Electronics in Agriculture, 97: 71-82. https://doi.org/10.1016/j.compag.2013.07.006
[67] Isotta, F.A., Frei, C., Weilguni, V., Perčec Tadić, M., Lassegues, P., Rudolf, B., Pavan, V., Cacciamani, C., Antolini, G., Ratto, S.M., Munari, M., Micheletti, S., Bonati, V., Lussana, C., Ronchi, C., Panettieri, E., Marigo, G., Vertačnik, G. (2014). The climate of daily precipitation in the Alps: Development and analysis of a high-resolution grid dataset from pan-Alpine rain-gauge data. International Journal of Climatology, 34(5): 1657-1675. https://doi.org/10.1002/joc.3794
[68] Wood, S.J., Jones, D.A., Moore, R.J. (2000). Accuracy of rainfall measurement for scales of hydrological interest. Hydrology and Earth System Sciences, 4(4): 531-543. https://doi.org/10.5194/hess-4-531-2000, 2000
[69] Syed, K.H., Goodrich, D.C., Myers, D.E., Sorooshian, S. (2003). Spatial characteristics of thunderstorm rainfall fields and their relation to runoff. Journal of Hydrology, 271(1-4): 1-21. https://doi.org/10.1016/S0022-1694(02)00311-6
[70] Singh, V.P. (1997). Effect of spatial and temporal variability in rainfall and watershed characteristics on stream flow hydrograph. Hydrological Processes, 11(12): 1649-1669. https://doi.org/10.1002/(SICI)1099-1085(19971015)11:12%3C1649::AID-HYP495%3E3.0.CO;2-1
[71] Cattle, J.A., McBratney, A.B., Minasny, B. (2002). Kriging method evaluation for assessing the spatial distribution of urban soil lead contamination. Journal of Environmental Quality, 31(5): 1576-1588. https://doi.org/10.2134/jeq2002.1576